Inventory of Supplemental Information

Supplementary Figures 1 and 2 are related to Figure 1.

Supplementary Figures 3 and 4 are related to Figure 2.

Supplementary Figure 5 is related to Figure 3.

Supplementary Figure 6 is related to Figure 5.

Supplementary Figure 7 is related to Figure 6.

Supplemental experimental procedures

Supplemental references

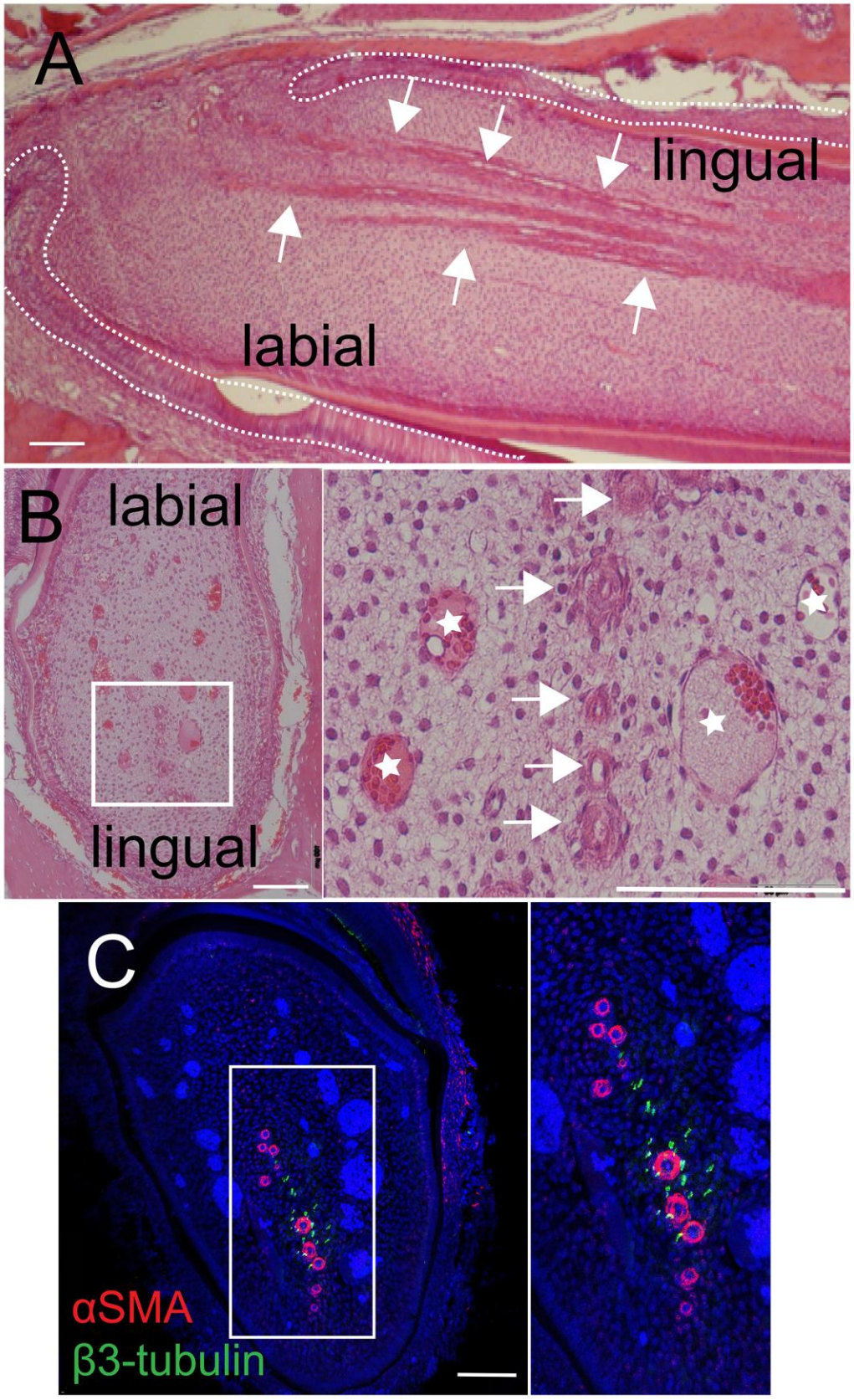
A
lingual
labial
B
labial
lingual
C
αSMA
β3-tubulin

Supplementary Figure 1. Structure of the neurovascular bundle in the adult incisor (related to Figure 1). A. HE staining of a sagittal section of an adult mouse incisor. Dotted lines outline dental epithelium. Arrows indicate arteries running in parallel towards the tip of the incisor (right side). B. HE staining of a cross section of an adult mouse incisor. Boxed area is enlarged in the right panel. Arrows indicate arteries bisecting the incisor. Stars indicate veins. C. αSMA (red) and β3-tubulin (green) immunofluorescence staining of a cross section of an adult mouse incisor indicating the companionship between arteries and nerves. Boxed area is enlarged in the right panel. Scale bars, 100μm.

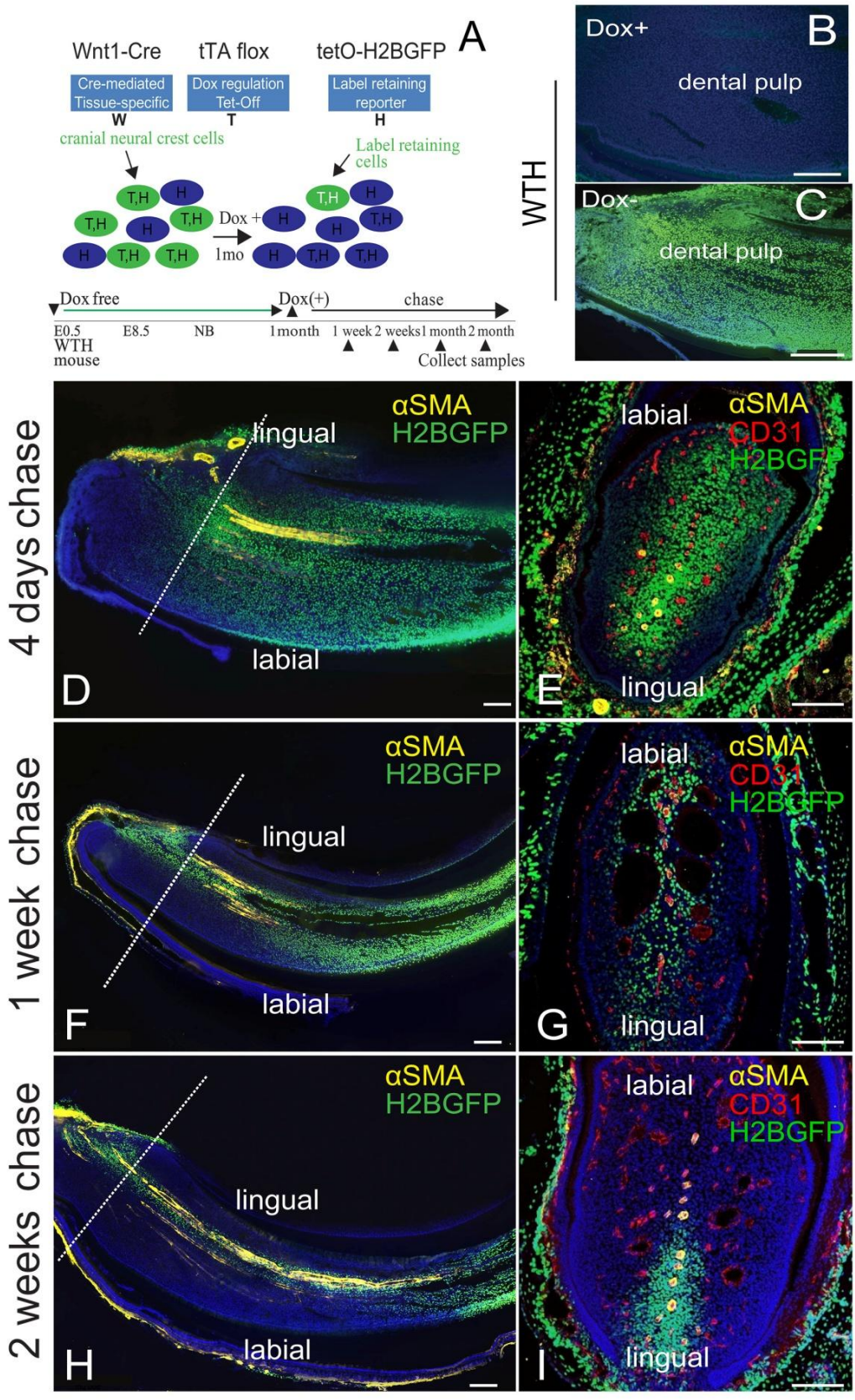
A
Wnt1-Cre
tTA flox
tetO-H2BGFP
Cre-mediated Tissue-specific
W
Dox regulation Tet-Off
T
Label retaining reporter
H
cranial neural crest cells
Label retaining cells
T,H
H
Dox +
1mo
Dox free
Dox(+)
chase
E0.5 WTH mouse
E8.5
NB
1month
1 week
2 weeks
1 month
2 month
Collect samples
WTH
B
Dox+
dental pulp
C
Dox-
dental pulp
4 days chase
1 week chase
2 weeks chase
αSMA
H2BGFP
CD31
lingual
labial
D
E
F
G
H
I

Supplementary Figure 2. Triple transgenic mouse model *Wnt1-Cre;ROSA26*$^{LoxP\text{-}STOP\text{-}LoxP\text{-}tTA}$*,tetO-H2BGFP* (WTH) to identify label retaining cells (LRCs) (related to Figure 1). A. In this model, H2BGFP expression is controlled by both neural crest tissue-specific Wnt1-Cre and the doxycyclin regulation element tTA. In the absence of doxycyclin, H2BGFP is expressed only in the neural crest-derived dental mesenchyme. Adding doxycyclin turns off *de novo* H2BGFP synthesis. Fast-dividing cells dilute the H2BGFP in the nucleus through cell division and only slow-cycling cells retain the H2BGFP label at the end of the chase period. B-C. Test of stringency of doxycyclin regulation in WTH mice. Sections of dental mesenchyme from WTH mice after feeding (B) or not feeding (C) doxycyclin from E0.5 to around 10 weeks of age. H2BGFP appears green. **D-I.** Time course study of WTH mouse incisors after addition of doxycyclin. αSMA (yellow) and CD31 (red) immunostaining of sagittal (D, F, H) and cross (E, G, I) sections of incisors from WTH mice fed with doxycyclin until 6-8 weeks of age, then chased for 4 days (D, E), 1 week (F, G) or 2 weeks (H, I). αSMA labels arteries. CD31 labels the vasculature. Dotted lines indicate the approximate position of the cross section. Scale bars, 100μm.

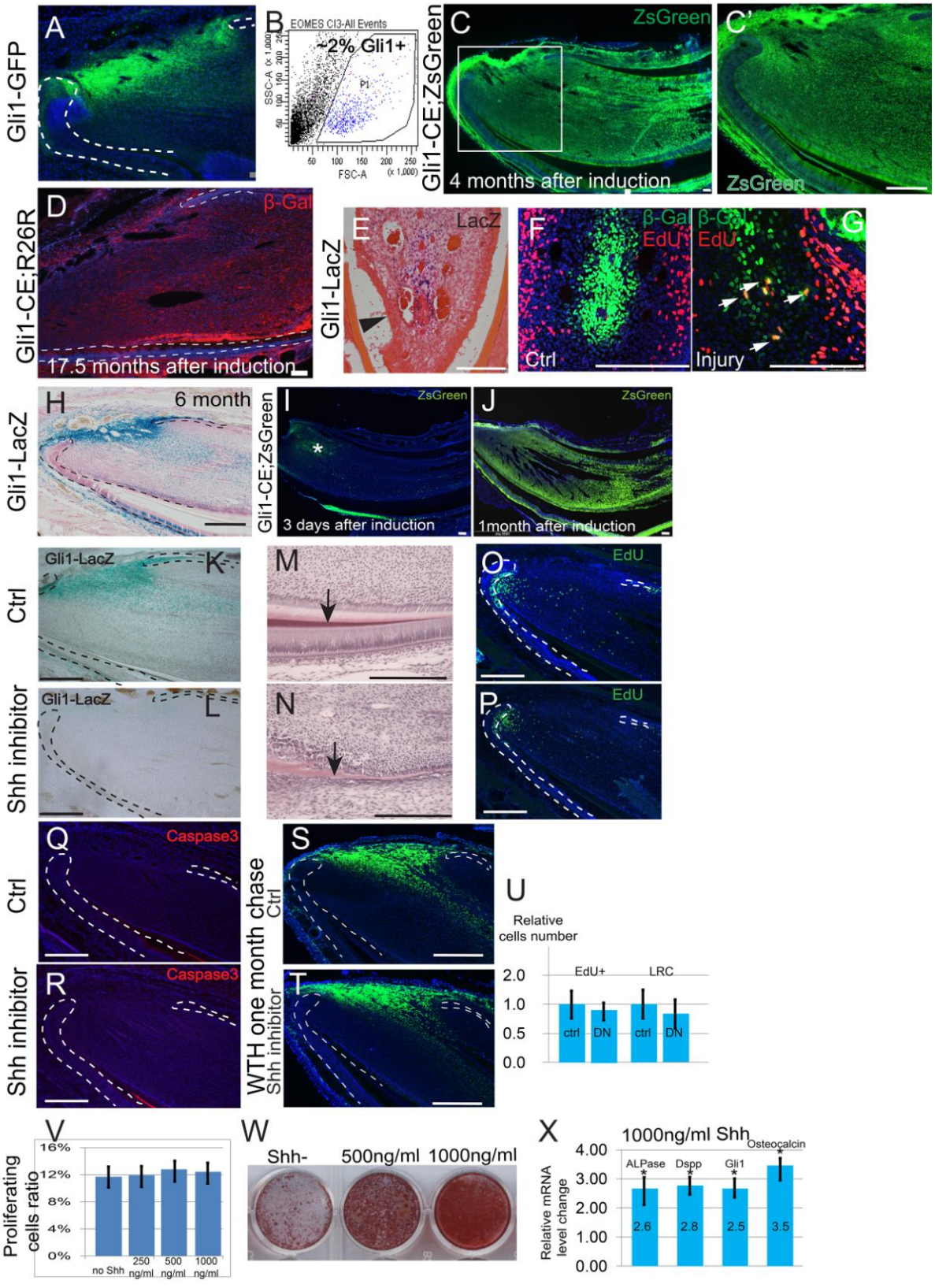
A
Gli1-GFP
B
EOMES CI3-All Events
~2% Gli1+
P1
SSC-A (x 1,000)
FSC-A (x 1,000)
C
ZsGreen
Gli1-CE;ZsGreen
4 months after induction
C'
ZsGreen
D
β-Gal
Gli1-CE;R26R
17.5 months after induction
E
LacZ
Gli1-LacZ
F
β-Gal
EdU
Ctrl
G
β-Gal
EdU
Injury
H
6 month
Gli1-LacZ
I
ZsGreen
Gli1-CE;ZsGreen
3 days after induction
J
ZsGreen
1month after induction
Gli1-LacZ
K
Ctrl
L
Shh inhibitor
M
N
O
EdU
P
EdU
Q
Caspase3
Ctrl
R
Caspase3
Shh inhibitor
S
WTH one month chase
Ctrl
T
Shh inhibitor
U
Relative cells number
EdU+
LRC
2.0
1.0
0.5
0.0
ctrl
DN
ctrl
DN
V
Proliferating cells ratio
16%
12%
8%
4%
0%
no Shh
250 ng/ml
500 ng/ml
1000 ng/ml
W
Shh-
500ng/ml
1000ng/ml
X
1000ng/ml Shh
Osteocalcin
Relative mRNA level change
4.00
3.00
2.00
1.00
0.00
ALPase
Dspp
Gli1
2.6
2.8
2.5
3.5

Supplementary Figure 3. A. Sagittal section of *Gli-GFP* mouse incisor at 1 month of age (related to Figure 2). B. FACS analysis conducted with cells harvested from *Gli1-GFP* mice incisors indicated that approximately 2% of cells in each lower incisor are Gli1+. C-D. Gli1+ cells continue to give rise to the entire dental mesenchyme 4 months and 17.5 months after induction. C. Visualization of incisors from *Gli1-CE;Zsgreen* mice 4 months after induction with tamoxifen. Tamoxifen was injected at around 4-6 weeks of age. Boxed area was magnified in the right panel (C'). D. β-Gal staining (red) of incisors from *Gli1-CE;ROSA26*$^{LoxP\text{-}STOP\text{-}LoxPLacZ}$ *(Gli1-CE;R26R*) mice 17.5 months after induction with tamoxifen. E. β-Gal staining (blue) of incisor from Gli1-LacZ mice 72 hours after injury (arrowhead indicates injury site). F,G Immunohistochemical staining with β-Gal and EdU of incisors from *Gli1-LacZ* mice before (F) and 24 hours after injury (G) indicates the activation of Gli1+ cells upon injury. Arrows indicate co-labeling of Gli1 and EdU. H-J. Gli1+ cells support incisor mesenchyme turnover. H. LacZ staining of *Gli1-LacZ* mouse incisor at 6 months of age. *Gli1-CE;ZsGreen* mice were induced with tamoxifen starting at 6 months of age and analyzed 72 hours (I) or 1 month later (J). Asterisk indicates ZsGreen positive cells in the mesenchyme. J. One month after induction ZsGreen+ cells were throughout the entire pulp, indicating that Gli1+ cells gave rise to the entire incisor mesenchyme. K-U. Effects of Shh inhibitor on incisor. Mice were fed with HhAntag continuously for 1 month and control mice were fed with vehicle. LacZ staining of inhibitor-treated *Gli1-LacZ* mice incisors (L) and control mouse incisors (K) indicates the inhibition of hedgehog activity in the incisor. HE staining indicated significantly reduced dentin formation in inhibitor-treated incisors (N) compared to control incisors (M). Black arrows indicate the dentin. EdU incorporation experiments indicated that proliferating cells in inhibitor-treated incisors (P) showed no difference from the controls (O). Results are quantified in (U) (n=3, p>0.05). Caspase 3 staining showed no apoptotic cells in either inhibitor-treated (R) or control incisors (Q). Adult WTH mice were chased for 1 month while being fed with vehicle or Shh inhibitor. The number of LRCs in inhibitor-treated incisors (T) was not significantly different from the controls (S). Results are quantified in (U). Values are plotted as mean ±SEM (n=3, p>0.05). V-X. Effects of Shh on incisor MSC *in vitro*. Cells harvested from adult mouse incisor mesenchyme were cultured in different concentrations of Shh. V. Ki67 staining was performed 10 days after plating and indicated that the percentage of proliferating cells in the presence of various concentrations of Shh was not significantly different from that in the controls. Values are plotted as mean ±SEM. (n=3, p>0.05). W. Incisor MSCs were subjected to osteogenic differentiation in the presence of 500ng/ml or 1000ng/ml of Shh. Alizarin red staining conducted 2 weeks later indicated enhanced calcified tissue formation in the Shh-treated dish with a dosage-dependent effect (W). X. Real-time PCR indicated that expression levels of odontogenic-related genes including ALPase, DsPP, Gli1 and Osteocalcin were significantly enhanced in the presence of 1000ng/ml Shh compared to the control culture. Values are plotted as mean ±SEM (*, p<0.01; n=4). White lines outline dental epithelium. Scale bars, 100 μm.

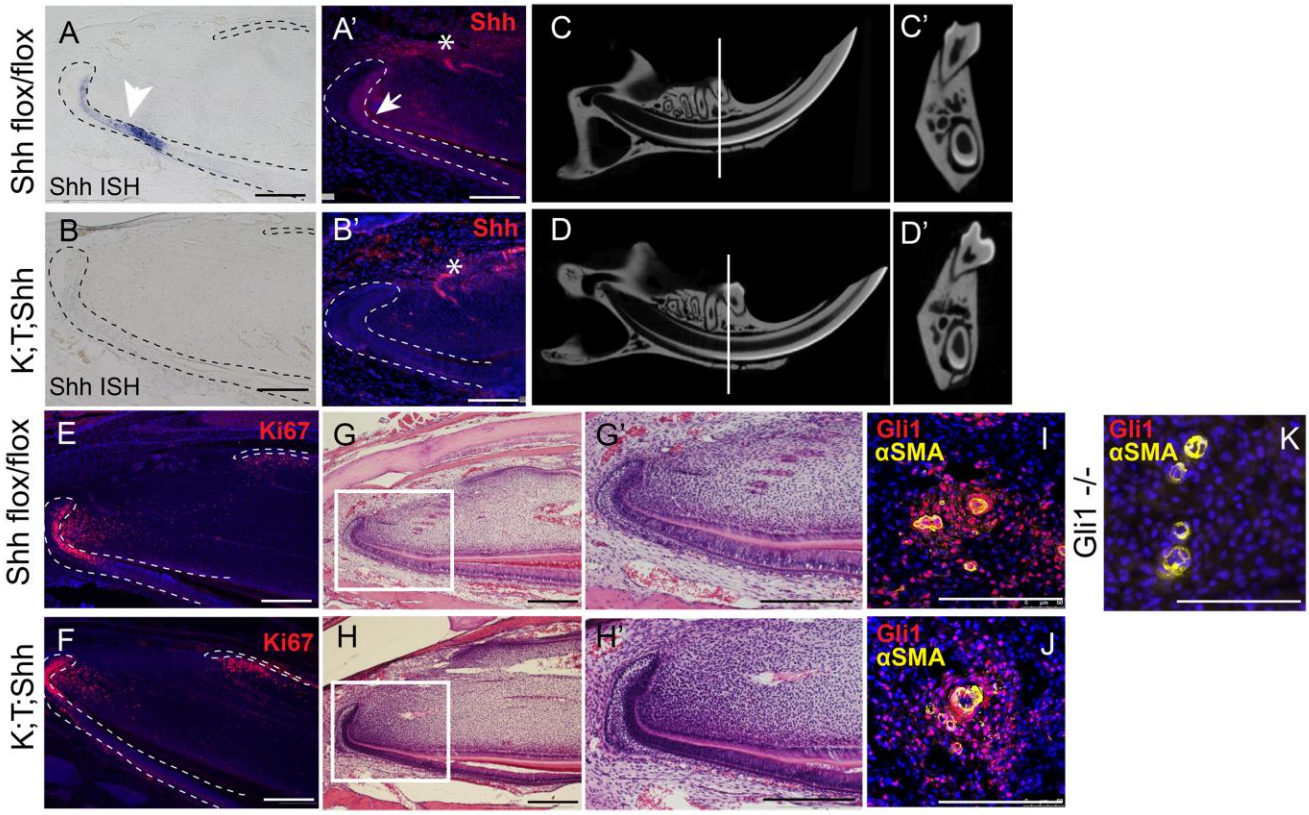

Supplementary Figure 4. Ablation of *Shh* from dental epithelium has no effects on odontogenesis or mesenchymal Gli1 expression (related to Figure 2). *K14-rtTA;tetO-Cre;Shh*$^{flox/flox}$ (*K;T;Shh*) mice at 1 month of age were fed with doxycyclin food for one month. Littermate mice of genotype *Shh*$^{flox/flox}$ were used as controls. Shh in the incisor epithelium was efficiently ablated (B) compared to the control (A). Immunohistochemical staining with Shh antibody confirmed Shh ablation in the dental epithelium whereas its presence in the mesenchyme was not affected (A', B'). White arrowheads indicate Shh expression in the epithelium. Asterisks indicate Shh expression in the mesenchyme. MicroCT sagittal (D) and cross sections (D') of *K;T;Shh* incisor show no significant difference from the control incisor (C, C'). White lines indicate the sample position of the cross sections. Ki67 staining showed no significant difference in proliferation between the control (E) and the *K;T;Shh* mutant (F) incisors. HE staining showed normal morphology and thickness of dentin in the mutant incisor (H, H') compared to the control (G, G'). Boxed areas are magnified in the right panels. Gli1 immunohistochemical staining showed a comparable number of Gli1+ cells surrounding arteries in *K;T;Shh* mutant (J) and control incisor (I) mesenchyme. To confirm the specificity of the Gli1 antibody, Gli1 immunohistochemical staining was performed on incisors of Gli1$^{-/-}$ mice, which showed no signal surrounding the NVB (K). Scale bars, 100 μm.

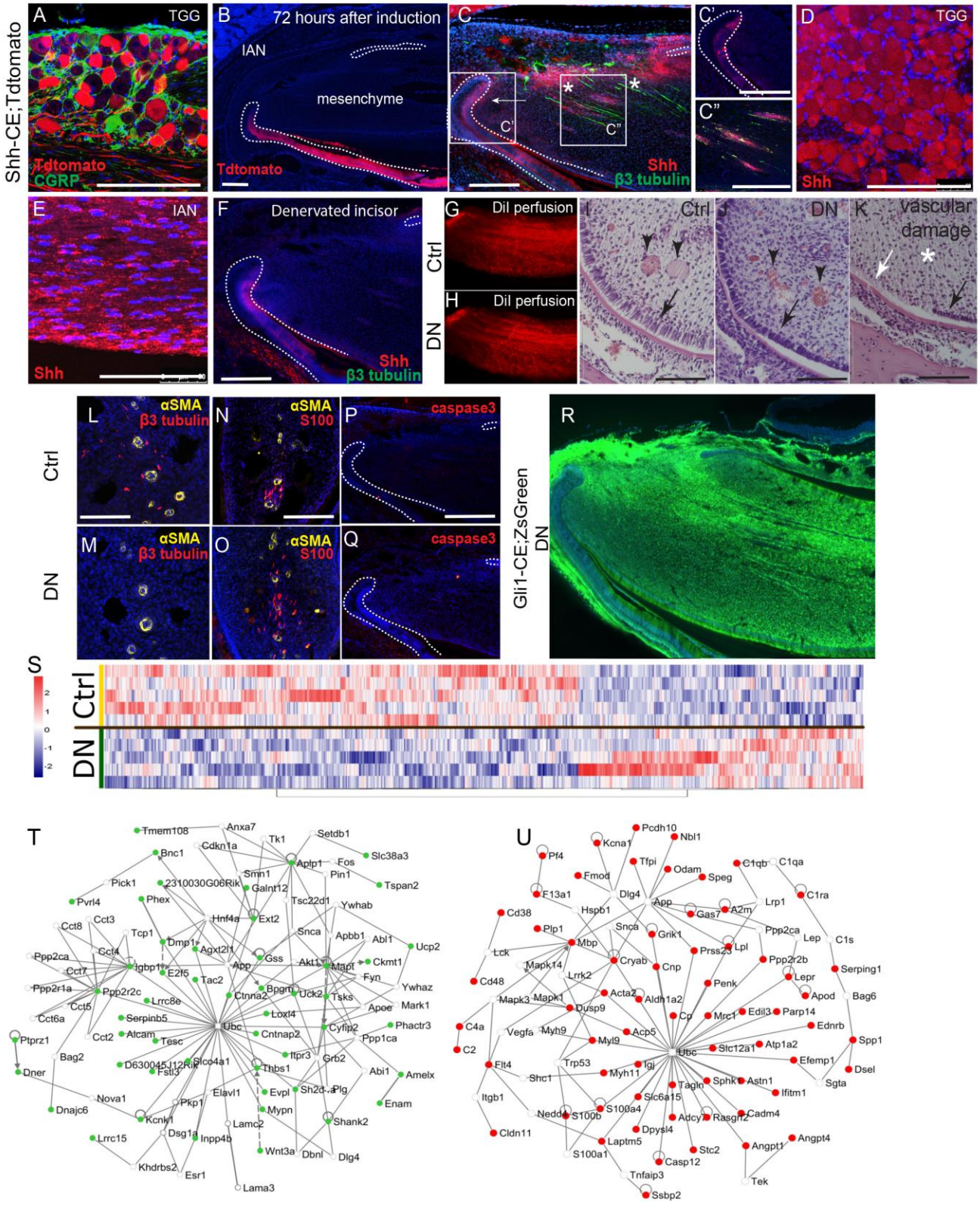
Shh-CE;Tdtomato
A
TGG
Tdtomato
CGRP
B
72 hours after induction
IAN
mesenchyme
Tdtomato
C
C'
C"
Shh
β3 tubulin
D
TGG
Shh
E
IAN
Shh
F
Denervated incisor
Shh
β3 tubulin
Ctrl
DN
G
DiI perfusion
H
DiI perfusion
I
Ctrl
J
DN
K
vascular damage
L
αSMA
β3 tubulin
M
αSMA
β3 tubulin
N
αSMA
S100
O
αSMA
S100
P
caspase3
Q
caspase3
Gli1-CE;ZsGreen
DN
R
S
Ctrl
DN
T
U

Supplementary Figure 5. Nerves provide Shh to incisor and denervation causes abnormal phenotypes (related to Figure 3). A-B. Trigeminal ganglion (TGG) and incisor were isolated from *Shh-CE;Tdtomato* mice 72 hours after tamoxifen induction. A. TGG was stained with sensory nerve marker CGRP (green). TdTomato fluorescence (red) indicates Shh activity. B. In the incisor, TdTomato fluorescence was observed in the labial side epithelium but not in the mesenchyme or the IAN. C. Shh immunohistochemical staining of incisors. Shh expression (red) was detected in the epithelium (C') and mesenchyme surrounding the nerve fibers (C''). Boxed area is magnified in the two right panels. Shh immunohistochemical staining also showed the presence of Shh protein in the TGG (D) and the IAN (E). Two weeks after denervation, Shh expression was only detected in incisor epithelium, not in the mesenchyme (F). G-H. DiI (red) was injected into the bloodstream of mice 24 hours after the denervation. Incisors from the control side (E) and denervated side (F) were dissected out and analyzed. HE staining was performed for incisors 72 hours after denervation (J) and on the control side (I). Arrowheads indicate red blood cells within the vasculature lumen. Arrows indicate normal odontoblast arrangement. As a control, HE staining was also performed on incisors 72 hours after the vasculature was damaged (K). Red blood cells are absent from the vasculature (asterisk) and white arrows indicate degenerated odontoblasts. β3 tubulin and S100 staining were performed 1 month after denervation for incisors on the control side (L, N) and the denervation side (M, O). Caspase 3 staining was performed 2 weeks after denervation on the control side (P) and denervated side (Q). White lines outline dental epithelium. R. Adult *Gli1-CE;ZsGreen* mice were induced with tamoxifen and then denervated 24 hours after the first induction. Samples were collected 1 month later. ZsGreen indicates cells derived from Gli+ cells. Scale bars 10μm. (S-U). Microarray analysis was performed on incisor pulp taken from 5 mice 2 weeks after denervation and incisors from the sham operation side were used as controls. (S). Heat map of relative expression for all transcripts (columns) with absolute fold-change greater than 1.25. The colored bars indicate standard deviations of expression with respect to the mean transcript expression over all samples (rows). Denervated incisors (DN) showed distinctive general transcript profiles from control (Ctrl) samples. The Ingenuity Pathway Analysis software (Ingenuity Systems, www.ingenuity.com) was used to construct networks of protein-protein interactions among downregulated genes (T) and upregulated genes (U) identified in this study. Unshaded nodes indicate molecules which were added to the networks to link additional genes.

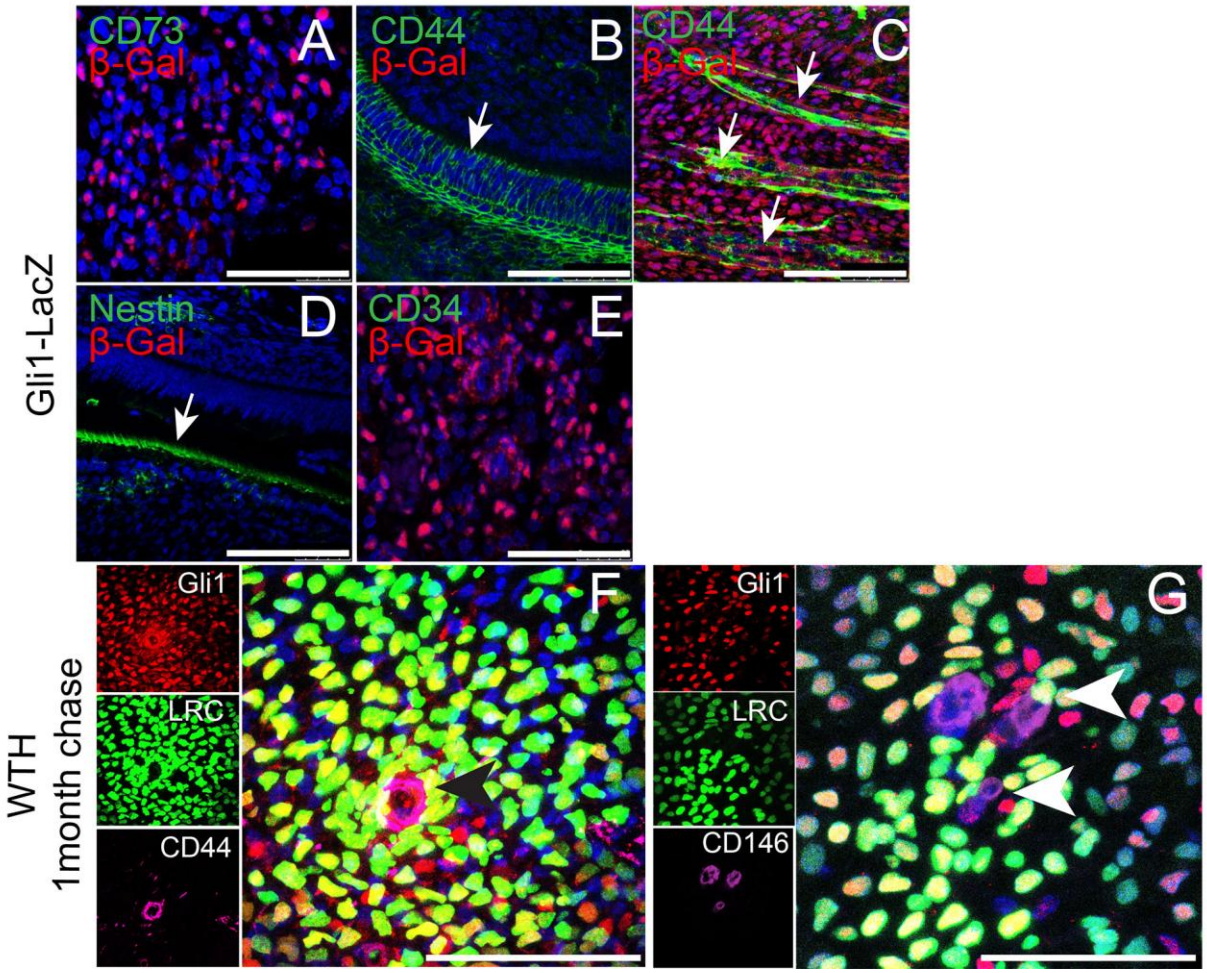

Supplementary Figure 6. Expression of MSC markers in Gli1+ cells (related to Figure 5). Incisors from *Gli1-LacZ* mice at 1 month of age were co-stained with β-Gal antibody (red) and surface marker antibodies (green). CD73 expression was not detected in the incisor mesenchyme (A). CD44 expression was detected in the dental epithelium (B) and surrounding the vasculature (C). The majority of Gli1+ cells do not express CD44 (C). Nestin expression was detected in odontoblasts located away from the cervical loop region where Gli1+ cells localized (D). CD34 expression was not detected in incisor mesenchyme or Gli1+ cells (E). F, G. Immunohistochemical staining of Gli1 and MSC markers CD44 (F) and CD146 (G) in incisors of WTH mice 1 month after chase. Arrowheads indicate co-labeling of all 3 markers. Scale bars, 100 μm.

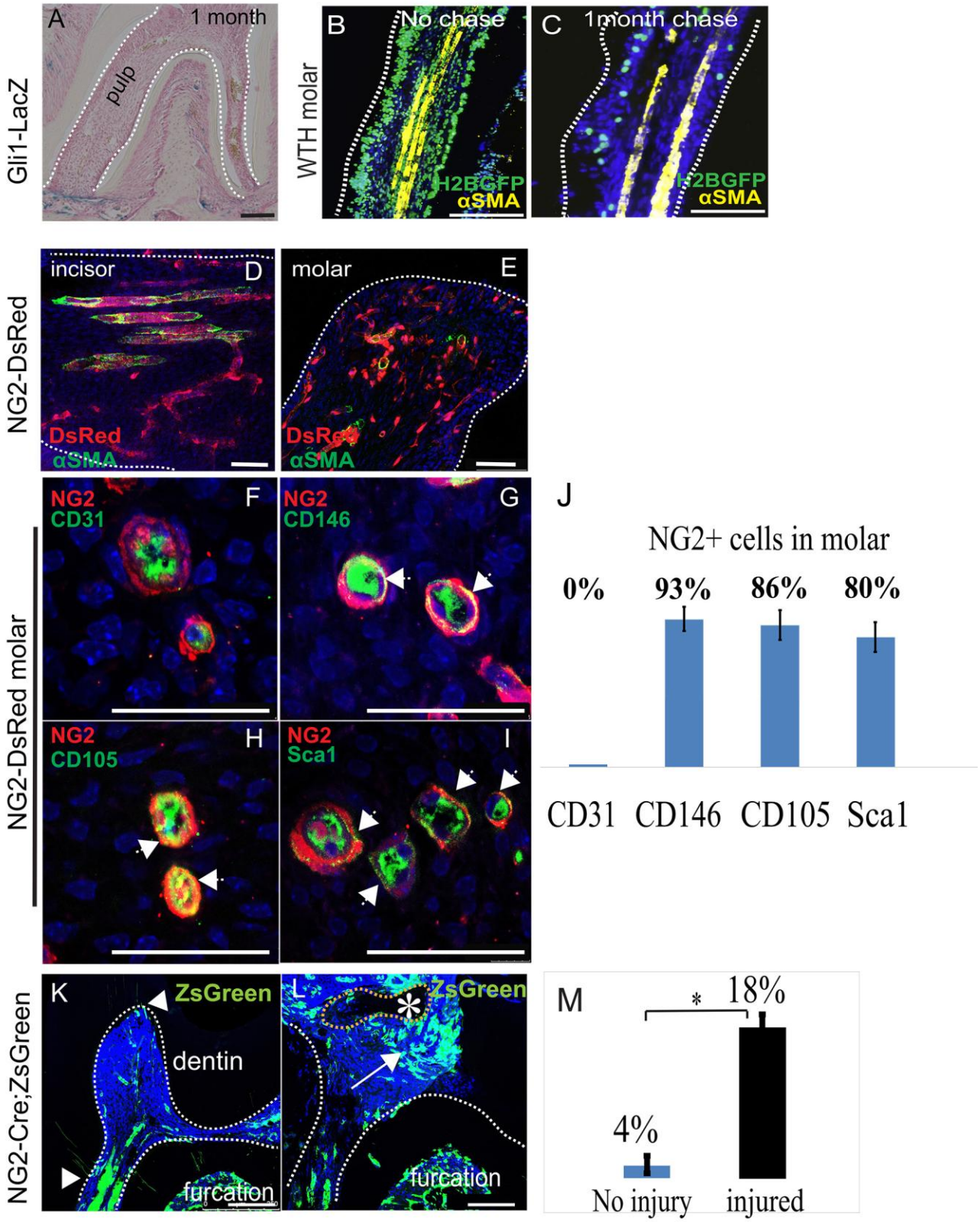
Gli1-LacZ
A
1 month
pulp
WTH molar
B
No chase
H2BGFP
αSMA
C
1month chase
H2BGFP
αSMA
NG2-DsRed
incisor
D
DsRed
αSMA
molar
E
DsRed
αSMA
NG2-DsRed molar
NG2
CD31
F
NG2
CD146
G
NG2
CD105
H
NG2
Sca1
I
J
NG2+ cells in molar
0%
93%
86%
80%
CD31
CD146
CD105
Sca1
NG2-Cre;ZsGreen
K
ZsGreen
dentin
furcation
L
ZsGreen
furcation
M
*
18%
4%
No injury
injured

Supplementary Figure 7. Gli1+ and NG2+ cells in mouse molars (related to Figure 6). LacZ staining of *Gli1-LacZ* mouse incisor at 1 month of age showed no Gli1+ cells in the molar mesenchyme (A). (B). Molars of WTH mice were chased for 1 month. (C). No label retaining cells (green) were detected surrounding the arteries labeled with αSMA staining (yellow). Teeth taken from *NG2-DsRed* mice at 1 month of age indicated that NG2+ cells were detected in all vasculature in the incisor (D) and molar (E). Arteries were labeled with aSMA (yellow). F-J. Immunohistochemical staining with CD31 and MSC markers was performed on *NG2-DsRed* mouse molars at one month of age. NG2+ cells are pericytes surrounding the endothelium (F). The majority of NG2+ cells in the molar express CD146 (G), CD105 (H) and Sca1 (I). Results are quantified in (J). Values are plotted as mean ±SEM (n=5). NG2-derived cells (green) in the incisor mesenchyme of untreated *NG2-Cre;ZsGreen* mice (K) or 3 weeks after injury (L) (n=4). Arrowheads indicate odontoblasts derived from NG2+ cells. Arrow indicates pulp cells derived from NG2+ cells. Asterisk indicates the reparative dentin. The percentage of NG2-derived odontoblasts is quantified in (M). Values are plotted as mean ±SEM (*, p<0.05, n=6).

Supplemental Table 1 (related to EXPERIMENTAL PROCEDURES)

Animal information

Mouse lines	**Source**	**References**
tetO-H2BGFP	Obtained from Dr. Agnieszka Kobielak (USC)	(Tumbar et al., 2004)
Wnt1-Cre	JAX #003829	(Danielian et al., 1998)
ROSA26$^{LoxP\text{-}STOP\text{-}LoxP\text{-}tTA}$	JAX#011008	(Wang et al., 2008)
Gli1-LacZ	JAX#008211	(Bai et al., 2002)
NG2-DsRed	JAX#008241	(Zhu et al., 2008)
Gli1-Cre^{ERT2}	JAX#007913	(Ahn and Joyner, 2004)
ROSA26$^{LoxP\text{-}STOP\text{-}LoxP\text{-}ZsGreen1}$	JAX#007906	(Madisen et al., 2010)
NG2-Cre	JAX#008533	(Zhu et al., 2008)
NG2-Cre^{ER}	JAX# 008538	(Zhu et al., 2011)
ROSA26$^{LoxP\text{-}STOP\text{-}LoxP\text{-}Tdtomato}$	JAX#007905	(Madisen et al., 2010)
ROSA26$^{LoxP\text{-}STOP\text{-}LoxPLacZ}$	JAX#003474	(Soriano, 1999)
ShhCre^{ERT2}	JAX#005623	(Harfe et al., 2004)
Gli1-GFP	Obtained from Dr. Alexandra Joyner (MSKCC)	(Brownell et al., 2011)
Shh$^{flox/flox}$	JAX#004293	(Lewis et al., 2001)
K14-rtTA	JAX#007678	(Xie et al., 1999)
tetO-Cre	JAX#006234	(Perl et al., 2002)

SUPPLEMENTAL EXPERIMENTAL PROCEDURES

MicroCT analysis

MicroCT analysis was performed using a SCANCO μCT50 device at the University of Southern California Molecular Imaging Center. The microCT images were acquired with the x-ray source at 70 kVp and 114 μA. The data were collected at a resolution of 10 μm. The three-dimensional (3D) reconstruction was done with AVIZO 7.1 (Visualization Sciences Group).

Flow cytometry analysis

Cultured incisor mesenchymal cells of p0 or p1 were stained with PE-conjugated antibodies of CD34, CD44, CD45, CD73, CD105, CD146, Sca1, CD130, CD271, or Nestin (BD Bioscience). All samples were analyzed with FACS^{calibur} (BD Bioscience).

Microarray analysis

Total RNA samples (1 μg per sample) were isolated from incisors and then converted into biotin-labeled cRNA using the GeneChip® IVT Labeling Kit and standard protocols recommended by Affymetrix (Santa Clara, CA, USA). Fragmented cDNA was applied to GeneChip® Mouse Genome 430 2.0 Arrays (Affymetrix) containing probe sets designed to detect over 39 000 transcripts. Probes sets showing ≥ 1.5-fold differential expression with a <5% FDR were identified using LIMMA (Linear Models for Microarray Data)-based linear model statistical analysis and FDR calculations were made using the SPLOSH (spacing's LOESS histogram) method. All scaled gene expression scores and .cel files are available at the National Center for Biotechnology Information (NCBI) Gene Expression Omnibus repository http://www.ncbi.nih.gov/geo/ under Series Accession Number GSE51479.

Real-time PCR primer sequences

Amelogenin	G A A A T G G G G A C C T G G A T T T T C C A C T T C A A A G G G G T A A G C A
Enamelin	C C A C A C C C A C T G A A A G T C C T C T T G G T C C T G T G G A C T G G T T
Dspp	GCTACACATGAAACGACGCC CCATCATGGCTCTCCCTTCC
Dmp	C G G C T G G T G G A C T C T C T A A G T G T C T G C C T C A T C C T C A C T G
Wnt3a	C C C T T T C C A G T C C T G G T G T A C T T G A A G A A G G G G T G C A G A G
Sfrp2	A G C C T G A G A A T C G G C A T C T A T A T T T G A G G G C A T C A T G C A A
Mbp	A T C C A A G T A C C T G G C C A C A G C C T G T C A C C G C T A A A G A A G C
S100b	G G A C A C T G A A G C C A G A G A G G T T C A G C T T G T G C T T G T C A C C
Gli1	G A A G G A A T T C G T G T G C C A T T G C A A C C T T C T T G C T C A C A C A
ALPase	CAGCGAGGGACGAATCTCAG CTGGCCCTTAAGGATTCGGG
Osteocalcin	A A G C A G G A G G G C A A T A A G G T C T T G C A G G G C A G A G A G A G A

Supplemental references:

Ahn, S., and Joyner, A.L. (2004). Dynamic changes in the response of cells to positive hedgehog signaling during mouse limb patterning. Cell *118*, 505-516.

Bai, C.B., Auerbach, W., Lee, J.S., Stephen, D., and Joyner, A.L. (2002). Gli2, but not Gli1, is required for initial Shh signaling and ectopic activation of the Shh pathway. Development *129*, 4753-4761.

Brownell, I., Guevara, E., Bai, C.B., Loomis, C.A., and Joyner, A.L. (2011). Nerve-derived sonic hedgehog defines a niche for hair follicle stem cells capable of becoming epidermal stem cells. Cell Stem Cell *8*, 552-565.

Danielian, P.S., Muccino, D., Rowitch, D.H., Michael, S.K., and McMahon, A.P. (1998). Modification of gene activity in mouse embryos in utero by a tamoxifen-inducible form of Cre recombinase. Curr Biol *8*, 1323-1326.

Harfe, B.D., Scherz, P.J., Nissim, S., Tian, H., McMahon, A.P., and Tabin, C.J. (2004). Evidence for an expansion-based temporal Shh gradient in specifying vertebrate digit identities. Cell *118*, 517-528.

Lewis, P.M., Dunn, M.P., McMahon, J.A., Logan, M., Martin, J.F., St-Jacques, B., and McMahon, A.P. (2001). Cholesterol modification of sonic hedgehog is required for long-range signaling activity and effective modulation of signaling by Ptc1. Cell *105*, 599-612.

Madisen, L., Zwingman, T.A., Sunkin, S.M., Oh, S.W., Zariwala, H.A., Gu, H., Ng, L.L., Palmiter, R.D., Hawrylycz, M.J., Jones, A.R.*, et al.* (2010). A robust and high-throughput Cre reporting and characterization system for the whole mouse brain. Nat Neurosci *13*, 133-140.

Perl, A.K., Wert, S.E., Nagy, A., Lobe, C.G., and Whitsett, J.A. (2002). Early restriction of peripheral and proximal cell lineages during formation of the lung. Proc Natl Acad Sci U S A *99*, 10482-10487.

Soriano, P. (1999). Generalized lacZ expression with the ROSA26 Cre reporter strain. Nat Genet *21*, 70-71.

Tumbar, T., Guasch, G., Greco, V., Blanpain, C., Lowry, W.E., Rendl, M., and Fuchs, E. (2004). Defining the epithelial stem cell niche in skin. Science *303*, 359-363.

Wang, L., Sharma, K., Deng, H.X., Siddique, T., Grisotti, G., Liu, E., and Roos, R.P. (2008). Restricted expression of mutant SOD1 in spinal motor neurons and interneurons induces motor neuron pathology. Neurobiol Dis *29*, 400-408.

Xie, W., Chow, L.T., Paterson, A.J., Chin, E., and Kudlow, J.E. (1999). Conditional expression of the ErbB2 oncogene elicits reversible hyperplasia in stratified epithelia and up-regulation of TGFalpha expression in transgenic mice. Oncogene *18*, 3593-3607.

Zhu, X., Bergles, D.E., and Nishiyama, A. (2008). NG2 cells generate both oligodendrocytes and gray matter astrocytes. Development *135*, 145-157.

Zhu, X., Hill, R.A., Dietrich, D., Komitova, M., Suzuki, R., and Nishiyama, A. (2011). Age-dependent fate and lineage restriction of single NG2 cells. Development *138*, 745-753.